

THE USE OF SHADOW-CASTING TECHNIQUE FOR MEASUREMENT OF THE WIDTH OF ELONGATED PARTICLES

I. OHAD, D. DANON, M.D., and S. HESTRIN, Ph.D.

From the Department of Biological Chemistry, Hebrew University, Jerusalem, Israel, and the Laboratory of Electron Microscopy, The Weizmann Institute of Science, Rehovoth, Israel

ABSTRACT

A method is described for the estimation of the true width of fibrillar or rod-like structures from electron micrographs of metal-shadowed preparations. The method is based on variations in the image width as a function of the angle (β) between the long axis of the fibril and the direction of the shadow in the plane of the preparation. The *image width* when $\beta = 0^\circ$ practically represents the real width of the elongated particle but is often indistinguishable from the background. The fibril *image width* is conveniently measured at β values between 15° and 90° . The true width is obtained by plotting the image width *versus* $\sin \beta$ and extrapolating to $\beta = 0^\circ$. Latex spheres are sprayed with the fibrils or rods to indicate the direction of shadow. Tobacco mosaic virus (TMV) was used as a model structure because of its known constant diameter of 150 Å (5). The width (in the case of TMV equal to the diameter) found by the present method was $150 \text{ Å} \pm 8 \text{ Å}$.

Since the introduction of the shadow-casting technique by Williams and Wyckoff (1) this technique has been widely used for visualization of very small particles of poor opacity to electrons and for measuring the height of particles above the surface of the supporting film. Hall (2, 3) extended the usefulness of this method to measuring diameters of spherical macromolecules as well as fibrillar macromolecules known to have a circular cross-section. However, when molecules or other fibrillar or rod-like structures are known or suspected to be of cross-section other than circular, it is difficult to obtain information about their width.

The difficulty in estimating the real width of a fibrillar structure resides in the correct appreciation of the width of metal (Fig. 1) added to the original structure by the casting of the metallic film. This added width can reach a value of $1/\tan \theta$ (θ being determined by the height to shadow ratio) multiplied by the thickness of the film (4) (Fig. 2). If the thickness of the film is between 10

and 20 Å and the height to shadow ratio is between 1/5 to 1/10, the added width will be between 50 and 200 Å, which can be a value considerably larger than the structure studied.

Another difficulty lies in recognizing the edge of the particle on the shadow side. This is especially true of fibrils or rods of cross-section other than rectangular, and can be overcome by casting a second shadow in an opposite direction (5, 6).

It is a common observation that the *image width* varies as a function of the angle (β) between the direction of the shadow and the long axis of the fibre (Figs. 1 and 3). The fibril *image width* is maximal at $\beta = 90^\circ$. It will gradually decrease as the value of β becomes smaller, until at very low values of β the image is often indistinguishable from the background (Fig. 3). The variation in the fibril *image width* is therefore correlated to the width of the metal deposited. The imperfection of the geometry of the metal evaporation system (7) causes a certain minimal width to be added

even at $\beta = 0^\circ$. Thus the measurement of the image width of conveniently discernible fibres yields results closest to the true value when $\beta = 0^\circ$ (see reference 3). At very low angles of β it is difficult to measure the width of the image of fibres below 50 A; it is, however, possible at angles between 15° and 90° (Fig. 3).

and the angle (β) (Fig. 1) between the long axis of the fibril or rod and the direction of shadow. For a given preparation, m , l , and θ are practically constant. It may be assumed ideally that the depth of the metallic "column" (Fig. 2), deposited on an infinitely small area, when measured in the direction of the evaporation source (e) (Fig. 2), depends

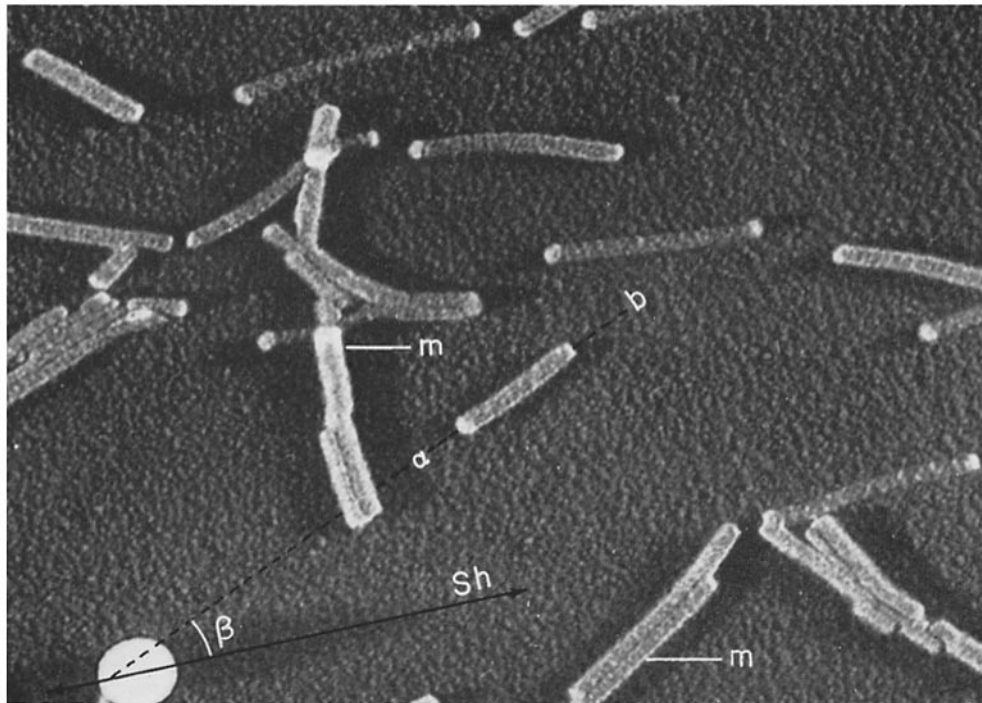


FIGURE 1
Tobacco mosaic virus double shadow cast by platinum. $\times 100,000$.
Sh, Shadow direction
a-b, long axis of the rod
 β , angle between the long axis of the rod and the shadow direction
m, metal added by shadow casting (bright)

In the present communication a method is described which enables the calculation of the *real width* of a fibril in the electron microscopic preparation from the variation in the observed *image width* as a function of the angle β .

THEORETICAL CONSIDERATIONS

The width of metal deposited on the side of a rod-like, or fibrillar, structure depends within the limits stated by Preuss (7) on the total mass of the evaporated metal (m), the distance of the particle from the source of evaporation (l), the angle (θ) determined by the height to shadow ratio (Fig. 2),

on m and l . The width of the added metal when measured perpendicularly to the long axis of the rod or fibril (b) (see Fig. 2) is equal to $f \cos \theta$. As θ is considered constant, b will therefore be only a function of $\sin \beta$ for angles other than $\beta = 90^\circ$.

The image width (Wi) is composed of the added metal (b) and the real width of the particle (k) (Fig. 2). Hence

$$(1) \quad Wi = b + k$$

and

$$(2) \quad b = f \cos \theta \cdot \sin \beta$$

The image width when $\beta = 0^\circ$ will represent the width of the rod-like or fibrillar particle. In this case

$$(3) \quad W_i = k$$

If shadow is cast from both sides, and $\beta = 90^\circ$

$$(4) \quad b = f \cos \theta$$

$$(5) \quad W_i = 2b + k$$

$$(6) \quad b = \frac{W_i - k}{2}$$

fibrils in the aggregate (n), plus twice the width of metal added by double shadowing ($2b$); $2b$ can of course be deduced by subtracting the product kn from the image width (W_i). The measurement of parallel aggregates represents a special case of an internal control when tobacco mosaic virus is used, such measurement not being an intrinsic requirement of the method. It is also evident that this method would be useful only in those cases in which the true width (k) is constant along the long axis of the particle.

FIGURE 2 Geometry of shadow casting from one direction.

e , evaporation source

θ , (height to shadow ratio) shadowing angle

l' , distance from projection of the evaporation source to the shadowed particle

f , depth of the metallic column, deposited on any small area of the preparation, measured in the direction of the evaporation source

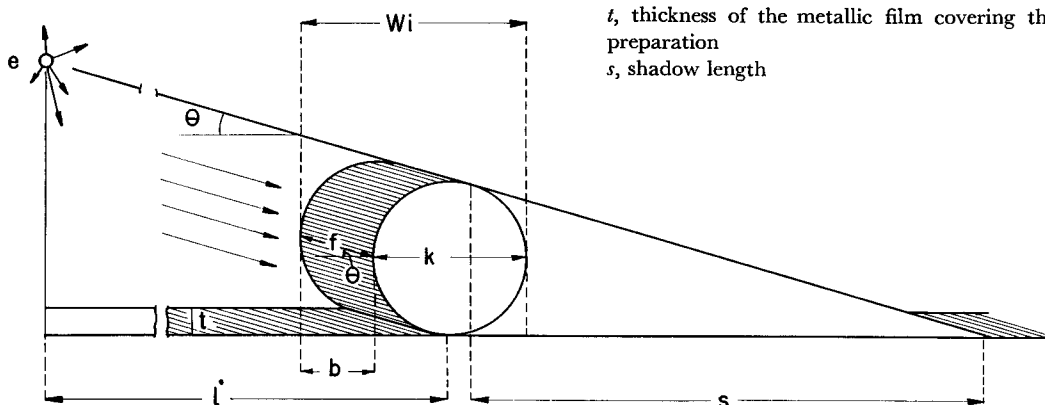
b , the width of the added metal measured perpendicularly to the long axis of the rod (equal to the projection of f in the horizontal plane)

k , diameter of the particle

W_i , width of the image of the shadowed particle

t , thickness of the metallic film covering the preparation

s , shadow length



The value of k can thus be theoretically calculated from Equation 6 by measuring two values of W_i at two β values between 15° and 90° . For better accuracy W_i is measured at various values of β between 15° and 90° . The value of k can then be deduced by extrapolation of W_i to $\beta = 0^\circ$, and will be determined by the intersection of the line obtained with the abscissa (Fig. 4).

From the above considerations, it is apparent that the dimensions of b are independent of the value of k . If this assumption is correct, when many rods or fibrils aggregate parallel to each other, and in the same plane with no gap between them, and $\beta = 90^\circ$, the width of the aggregate should be k multiplied by the number of rods or

EXPERIMENTAL

Tobacco mosaic virus (TMV)¹ was used as a model structure because of its known and constant diameter (150 A) (5). The virus was suspended in distilled water at a concentration of 50 μg dry weight/ml, mixed with Dow latex spheres and sprayed by means of a nebulizer (Vaponefrin Co., Upper Darby, Pennsylvania) onto the surface of a freshly cleaved mica strip (2).

After air drying at room temperature, the preparations were shadowed with platinum at a height to

¹ Kindly supplied by Dr. G. Lowenstein, Institute of Agriculture Research, Beit Dagon, Israel.

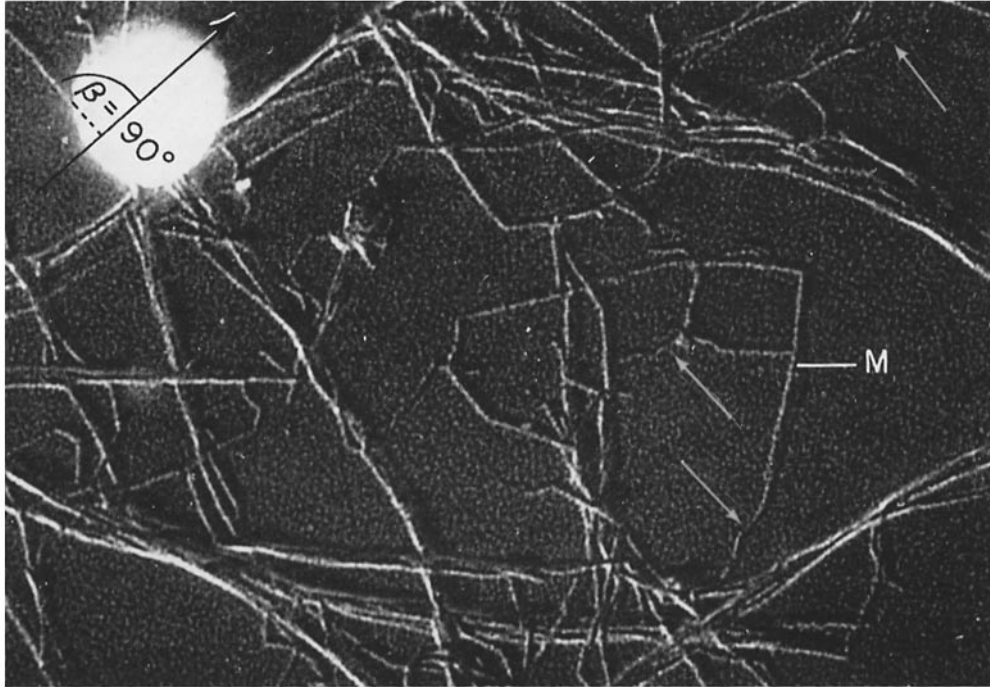


FIGURE 3

Cellulose microfibrils.

Cellulose was isolated from 3-day-old corn coleoptiles (14) and dispersed by sonication in a 10 kc Raytheon apparatus for 30 minutes. Samples containing 50 μg dry weight/ml were mixed with latex spheres (0.184 μ diameter, Dow Chemical Corp.) and sprayed on a freshly cleaved mica surface. The preparation was shadowed with platinum at 1/5 height to shadow ratio and further processed as described under Experimental. $\times 100,000$.

Microfibrils (*M*) are easily seen at $\beta > 15^\circ$ but practically undiscernible from background at $\beta < 15^\circ$ (arrows).

shadow ratio of 1 to 5 or 1 to 6. A platinum wire, 0.19 mm in diameter and 8 mm in length, was evaporated from a helix type source to yield the desired thickness of metallic film (8), from a height of 1.6 cm and a distance of 8 or 10 cm from the centre of the specimen. Some of the preparations were then turned through 180° and reshadowed at the same height to shadow ratio. The shadowed material was coated with a thin layer of carbon and reinforced with collodion. After floating and mounting on copper grids, the preparations were observed with an RCA EMU 3B electron microscope. Areas of field were arbitrarily chosen with particles spread in such a manner as to permit the measurement of about 15 values of β on different single rods.

Measurement of *image width* (W_i) was made perpendicularly to the long axis of the particle on negative micrographs at a magnification of 16,000 or 32,000, with a binocular microscope ($\times 50$) fitted

with a scale (each division 0.02 mm) and a protractor. The angle β for each particle was measured with reference to the latex sphere shadow direction within $\pm 2^\circ$ as shown in Fig. 1.

RESULTS

The diameter of TMV rods calculated from the shadow length was found to be $154 \text{ \AA} \pm 7 \text{ \AA}$. Their measured *image width* (W_i) was 380 \AA at $\beta = 90^\circ$, 300 \AA at $\beta = 45^\circ$, and 210 \AA at $\beta = 15^\circ$. The real width (in the case of TMV, equal to the diameter) was obtained by extrapolation to $\beta = 0^\circ$. The data for drawing the extrapolation curves were obtained from the same area of a preparation. The intersection points indicated a real width of $150 \text{ \AA} \pm 8 \text{ \AA}$ (Fig. 4).

The width of the metal added from both sides at

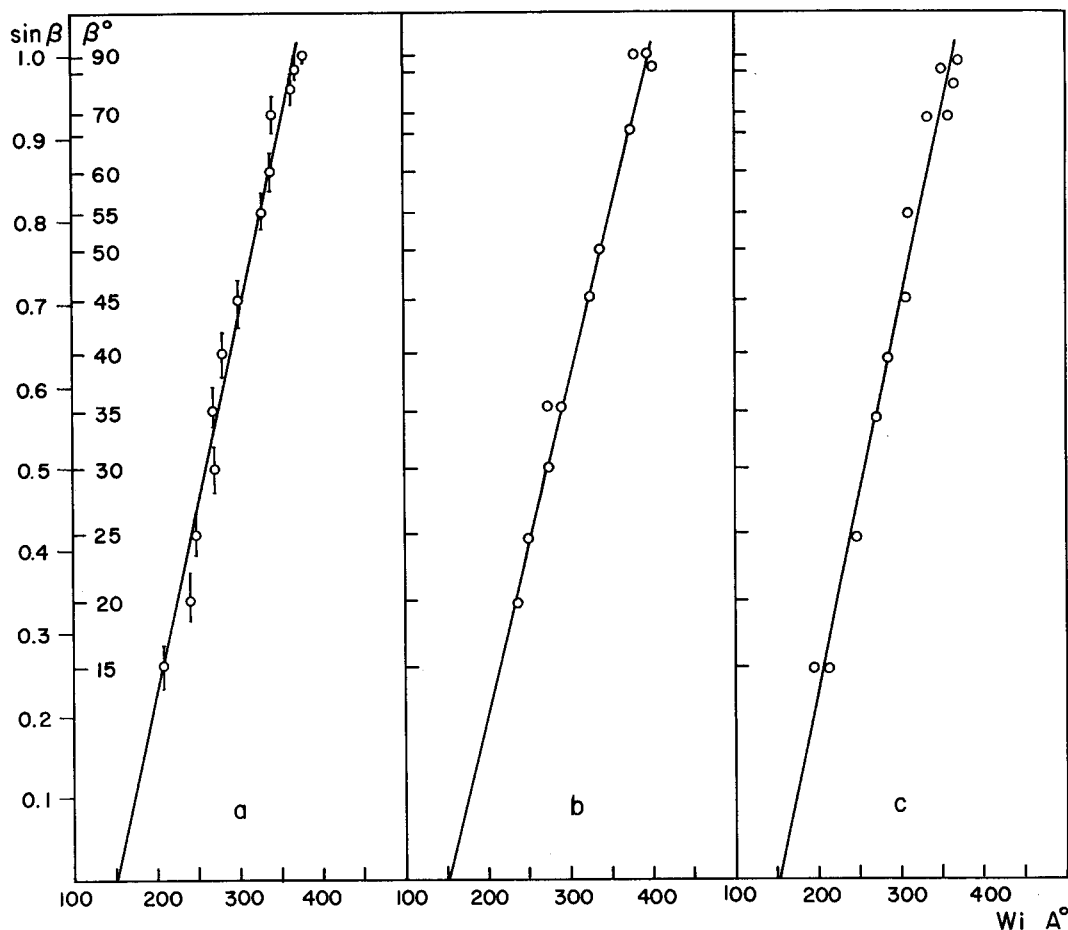


FIGURE 4

Plots of image width (W_i) versus $\sin \beta^\circ$. The data for plot (a) were obtained from 10 different micrographs and represent mean values. The data for plots (b) and (c) were obtained from two consecutive micrographs from the same field. Only one point is marked for a given value of β if the two measurements coincide.

$\beta = 90^\circ$ was calculated to be about 230 A; *i.e.*, 115 A on each side. This was further confirmed by measuring the *image width* of parallel virus aggregates at $\beta = 90^\circ$. The added width of metal calculated from the electron micrographs varied between 200 A and 250 A for aggregates containing from 2 to 6 virus particles, and was thus practically independent of the width of the structure studied, as expected (Table I).

The image width of a single straight rod measured at 5 different points was constant within $\pm 3\%$, which is within the accuracy of the measurement method. The same variation was found between sets of measurements of rods from the same preparation.

TABLE I
The Increase in Width by the Metal Added by Double Shadowing of Virus Aggregates

Measured values		Calculated values (in A)	
No. of rods in the aggregate (n)	Width of the image in A (W_i)	Expected real width (virus diameter k) times n (kn)	The part of the added metal, by double shadowing, in the image width
2	520	300	220
3	680	450	230
4	815	600	215
5	950	750	200
6	1150	900	250

DISCUSSION

The slight discrepancy between the diameter of the particles as calculated from the shadow length and as calculated according to the method described above may be accounted for by the difficulty in the exact measurement of the shadow length. The difference between the two methods is not greater than 3 per cent.

The fact that the added metal width when calculated from measurements of aggregates of virus rods varies between 200 Å and 250 Å may be explained by the different distances between the central axis of the rods that can occur in TMV aggregates (5, 9).

Images of metal-shadowed fibrils which are 0.1 to 0.5 μ m in width on micrographs or negatives can be easily employed for extrapolating the real width as described. The accuracy of the method would be dependent on the proper determination of the shadow direction and measurement of the apparent width (W_i). Thus technical details such as metal grain and geometry of shadowing should be considered.

The width of shadowed microfibrils obtained from a variety of biological systems measured on electron micrographs has been found by many workers to be 100 to 250 Å. This has been considered as the true fibre width (see references 10 and 11). A reconsideration of existing micrographs of metal-shadowed fibrils might provide more accurate information on their real width. With

the method described above, the real width of native bacterial cellulose was found to be about 30 Å (11).

Methods have been developed recently which enable the measurement of the width of fine fibrils, such as the phosphotungstic acid (PTA) negative staining method (12). When the PTA was used for the study of cellulose microfibrils (13, 14), the results obtained were similar to those found by the extrapolation method. Nucleic acid and other negatively charged fibrillar molecules can be stained by heavy metal salts (15, 16), and measured on electron micrographs. The advantage of the present method is in the convenient visualization of fibrils in the range below 3 μ m and the possibility of measuring the thickness and width of a structure on the same electron micrograph, under the same experimental conditions. It is not limited to molecules that are negatively charged or to structures that are impermeable to PTA or other heavy metal salts.

Dr. Hestrin died on February 2, 1962, after the work for this paper had been completed. Experiments presented in this communication are a part of a Ph.D. thesis being submitted by I. Ohad to the Hebrew University, Jerusalem.

This investigation was partially supported by a research grant (E-1494) from the National Institute of Allergy and Infectious Diseases of the National Institute of Health, United States Public Health Service, Bethesda, Maryland.

Received for publication, September 27, 1962.

REFERENCES

1. WILLIAMS, R. C., and WYCKOFF, R. W. G., *J. Appl. Physics*, 1944, **15**, 712.
2. HALL, C. E., *J. Biophysic. and Biochem. Cytol.*, 1956, **2**, 625.
3. HALL, C. E., *J. Biophysic. and Biochem. Cytol.*, 1960, **7**, 613.
4. HALL, C. E., *Introduction to Electron Microscopy*, New York, McGraw Hill Book Co., Inc., 1953, 336.
5. KAHLER, H., and LLOYD, B. J. JR., *J. Appl. Physics*, 1950, **21**, 699.
6. VOGEL, A., Ph.D. thesis, Hochschule, Zurich, Dr. A. Hühig, Verlag Heidelberg, 1953.
7. PREUSS, L. E., *RCA Scient. Inst. News*, 1959, **4**, 7.
8. DANON, D., data to be published.
9. BERNAL, J. D., and FANKUCHEN, I., *J. Gen. Physiol.*, 1942, **25**, 111.
10. BALASHOV, V., and PRESTON, R. D., *Nature*, 1955, **176**, 64.
11. OHAD, I., DANON, D., and HESTRIN, S., *J. Cell Biol.*, 1962, **12**, 31.
12. BRENNER, S., and HORNE, R. W., *Biochim. et Biophysica Acta*, 1959, **34**, 103.
13. MÜHLETHALER, K., *Z. Schwiez. Forstv.*, 1960, **30**, 55.
14. OHAD, I., DANON, D., and HESTRIN, S., data to be published.
15. BEER, M., and ZOBEL, R., *J. Mol. Biol.*, 1961, **3**, 717.
16. STOECKENIUS, W., *J. Biophysic. and Biochem. Cytol.*, 1961, **11**, 237.